

Structural and Solvent Effects on the C–S Bond Cleavage in Aryl Triphenylmethyl Sulfide Radical Cations

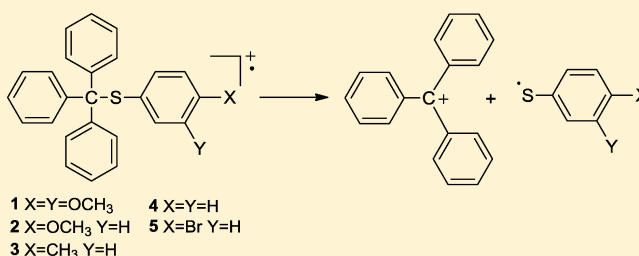
Tiziana Del Giacco,^{*,‡} Osvaldo Lanzalunga,^{*,†} Marco Mazzonna,[†] and Paolo Mencarelli^{*,†}

[†]Dipartimento di Chimica and Istituto CNR di Metodologie Chimiche-IMC, Sezione Meccanismi di Reazione c/o Dipartimento di Chimica, Sapienza Università di Roma, P.le A. Moro 5, 00185 Rome, Italy

[‡]Dipartimento di Chimica and Centro di Eccellenza Materiali Innovativi Nanostrutturati, Università di Perugia, via Elce di Sotto 8, 06123 Perugia, Italy

S Supporting Information

ABSTRACT: Steady-state and laser flash photolysis (LFP) studies of a series of aryl triphenylmethyl sulfides [1, 3, 4- $(\text{CH}_3\text{O})_2\text{-C}_6\text{H}_3\text{SC}(\text{C}_6\text{H}_5)_3$; 2, 4- $\text{CH}_3\text{O-C}_6\text{H}_4\text{SC}(\text{C}_6\text{H}_5)_3$; 3, 4- $\text{CH}_3\text{-C}_6\text{H}_4\text{SC}(\text{C}_6\text{H}_5)_3$; 4, $\text{C}_6\text{H}_5\text{SC}(\text{C}_6\text{H}_5)_3$; and 5, 4- $\text{Br-C}_6\text{H}_4\text{SC}(\text{C}_6\text{H}_5)_3$] has been carried out in the presence of *N*-methoxyphenanthridinium hexafluorophosphate in CH_3CN , CH_2Cl_2 , $\text{CH}_2\text{Cl}_2/\text{CH}_3\text{CN}$, and $\text{CH}_2\text{Cl}_2/\text{CH}_3\text{OH}$ mixtures. Products deriving from the C–S bond cleavage in the radical cations $1^{\bullet+}$ – $5^{\bullet+}$ have been observed in the steady-state photolysis experiments. Time-resolved LFP showed first-order decay of the radical cations accompanied by formation of the triphenylmethyl cation. A significant decrease of the C–S bond cleavage rate constants was observed by increasing the electron-donating power of the arylsulfenyl substituent, that is, by increasing the stability of the radical cations. DFT calculations showed that, in $2^{\bullet+}$ and $3^{\bullet+}$, charge and spin densities are mainly localized in the ArS group. In the TS of the C–S bond cleavage an increase of the positive charge in the trityl moiety and of the spin density on the ArS group is observed. The higher delocalization of the charge in the TS as compared to the initial state is probably at the origin of the observation that the C–S bond cleavage rates decrease by increasing the polarity of the solvent.



INTRODUCTION

Among the different classes of radical cations, sulfur radical cations are of particular importance not only for practical and theoretical aspects¹ but also for their involvement in biological oxidation processes.²

Depending on the structure and the experimental conditions, sulfide radical cations might undergo several reactions. C–S fragmentation to form an alkyl cation and a sulfenyl radical (eq 1) is certainly one of the most studied decomposition pathways of these species.³



These reactions are of particular interest since they can have important applications as in coal desulfurization processes.⁴ In addition, the detection of fragmentation products can provide information on whether radical cations are formed as intermediates in chemical and biological oxidation of sulfur compounds.⁵

An interesting characteristic of the C–S bond cleavage in aromatic sulfide radical cations (eq 1, R' = aryl) is represented by the fact that the cleaved C–S bond is α to the SOMO which is mostly located on the sulfur atom (α -fragmentation). This behavior differs from what observed in C–H, C–C, and C–Si bond cleavages in aromatic radical cations where the scissile

bond is β with respect to the SOMO which is delocalized in the aromatic ring (β -fragmentation).⁶

The quantitative aspects of the C–S bond cleavage in aromatic sulfide radical cations have been analyzed in detail by our research group by steady-state and laser photolysis studies of *tert*-alkyl aryl sulfide radical cations ($\text{ArSCR}_3^{\bullet+}$) where no competition with β -C–H bond cleavage reaction is possible. The effect of the structure of the *tert*-alkyl group on the rate of the C–S bond cleavage was analyzed using a series of phenyl sulfides: $(\text{CH}_3)_3\text{CSPH}$, PhMe_2CSPH , Ph_2MeCSPH , and Ph_3CSPH .⁷ It was found that the fragmentation rates were not particularly fast, depending to a very limited extent on the strength of the C–S bond in the radical cation, ranging from $6.6 \times 10^4 \text{ s}^{-1}$ for $\text{PhMe}_2\text{CSPH}^{\bullet+}$ to $9.5 \times 10^6 \text{ s}^{-1}$ for $\text{Ph}_3\text{CSPH}^{\bullet+}$. The results of this investigation suggested that the C–S bond scission is characterized by a large reorganization energy; moreover, steric effects might play a significant role on the rate of this process.

More recently, information on the electronic effects of substituents in the alkyl group on the rates of C–S bond cleavage have been obtained by the analysis of a series of aryl cumyl sulfide radical cations ($4\text{-X-C}_6\text{H}_4\text{C}(\text{CH}_3)_2\text{SC}_6\text{H}_5^{\bullet+}$) presenting the same steric situation at the scissile bond.⁸ The

Received: November 30, 2011

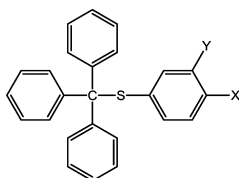
Published: January 12, 2012



rates of C–S bond cleavage were relatively low and very little sensitive to the nature of the substituent. Only a modest increase was observed from the lowest ($3.6 \times 10^4 \text{ s}^{-1}$ for $X = \text{Br}$) to the highest ($4.5 \times 10^5 \text{ s}^{-1}$ for $X = \text{OCH}_3$) fragmentation rate. On the basis of the results of DFT calculations it was suggested that the significant delocalization of charge and spin densities in the thiophenolic group and the cumyl ring is probably at the origin of the small effect of the substituents on the rates of C–S bond cleavage. By applying the Marcus equation a large reorganization energy could be estimated for this process, which is intrinsically much slower than C–C bond cleavage in bicumyl radical cations.⁹

Along this line, we have considered it worthwhile to extend the analysis of the substituents effect on the C–S bond cleavage in radical cations of aromatic sulfides by changing the substituents in the arylsulfonyl ring where the radical cation should be mostly localized.¹⁰ We now report on a steady-state and laser photolysis study of the C–S bond cleavage of the radical cations of a series of aryl triphenylmethyl sulfides (**1–5**).

These compounds are particularly suitable for the investigation of the C–S bond-cleavage processes by LFP studies. Accordingly, the decay of the radical cation is accompanied by the formation of the trityl cation, which is characterized by an intense absorption band at 400–430 nm.^{7,11} Thus, the C–S fragmentation of the radical cations **1^{•+}–5^{•+}** can be easily monitored by following either the decay of **1^{•+}–5^{•+}** or the buildup of $(\text{C}_6\text{H}_5)_3\text{C}^+$. The effect of the solvent polarity has been also investigated by determining the C–S fragmentation rates in CH_3CN and CH_2Cl_2 and in the solvent mixtures $\text{CH}_2\text{Cl}_2/\text{CH}_3\text{CN}$ and $\text{CH}_2\text{Cl}_2/\text{CH}_3\text{OH}$.



- | | |
|---|------------------------|
| 1 | X=Y=OCH ₃ |
| 2 | X=OCH ₃ Y=H |
| 3 | X=CH ₃ Y=H |
| 4 | X=Y=H |
| 5 | X=Br Y=H |

This study has been integrated by DFT calculations at the B3P86/6-311+G(d,p) level of theory for sulfides **2** and **3**, which provided us the C–S bond dissociation energy values (BDEs) that have been used to determine the bond dissociation free energies (BDFEs) in the corresponding radical cations **2^{•+}–3^{•+}**. DFT calculations at the B3LYP/6-311G(d,p) level of theory have been also carried out for radical cations **2^{•+}–3^{•+}** in order to get information on the geometry, charge, and spin distribution of the radical cations. Calculations allowed, for the first time, to identify the structure, charge, and spin

distribution and relative energies of the transition states for the C–S bond cleavage process of the two radical cations.

RESULTS

The method used for the photochemical generation of radical cations **1^{•+}–5^{•+}** was the same as reported previously^{7,8} and is based on the light-induced N–O bond cleavage in the *N*-methoxyphenanthridinium cation (**MeOP⁺**).¹² The phenanthridinium radical cation (**P^{•+}**) formed is a quite powerful oxidant ($E^\circ = 1.9 \text{ V vs SCE}$) able to oxidize the aromatic sulfides which are characterized by oxidation potentials around or lower than 1.6 V vs SCE¹³ (Scheme 1).

Steady-State Photolysis. Steady-state photolysis experiments were carried out by irradiating a solution of sulfides **1–5** ($2.5\text{--}25 \times 10^{-3} \text{ M}$) in N_2 -saturated CH_3CN , CH_2Cl_2 , and $\text{CH}_2\text{Cl}_2/\text{CH}_3\text{OH}$ 1:1 at around 355 nm, in the presence of **MeOP⁺PF₆[−]** ($0.5\text{--}2.5 \times 10^{-3} \text{ M}$). The molar ratio sulfides/**MeOP⁺** was 5:1 in all the experiments. Reaction products were identified and quantified by HPLC analysis by comparison with authentic specimens. No products were detected without irradiation or in the absence of the sensitizer.

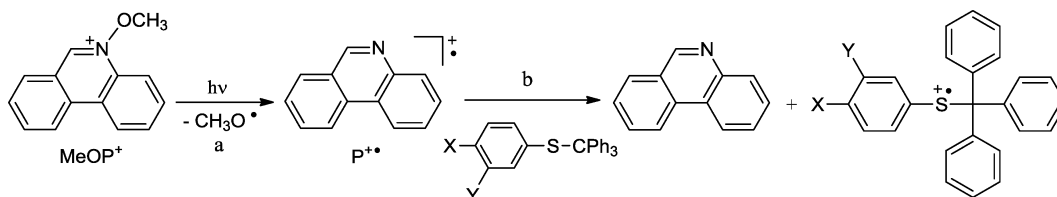
The photolysis of sulfides **1–5** produced in substantial amounts the fragmentation products diaryl disulfide from the sulfide moiety and triphenylmethanol, in CH_3CN and CH_2Cl_2 , or methyl triphenylmethyl ether, in the solvent mixture $\text{CH}_2\text{Cl}_2/\text{CH}_3\text{OH}$, from the alkyl group. Other products observed were those deriving from the N–O fragmentation of the **MeOP⁺** (protonated phenanthridine, **PH⁺** and methanol) (Scheme 2).

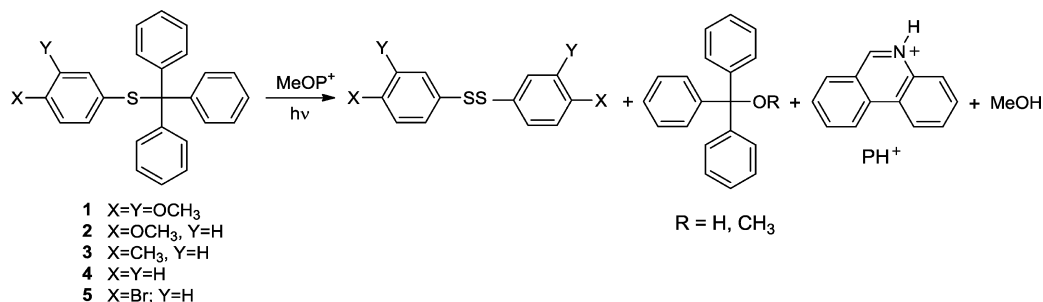
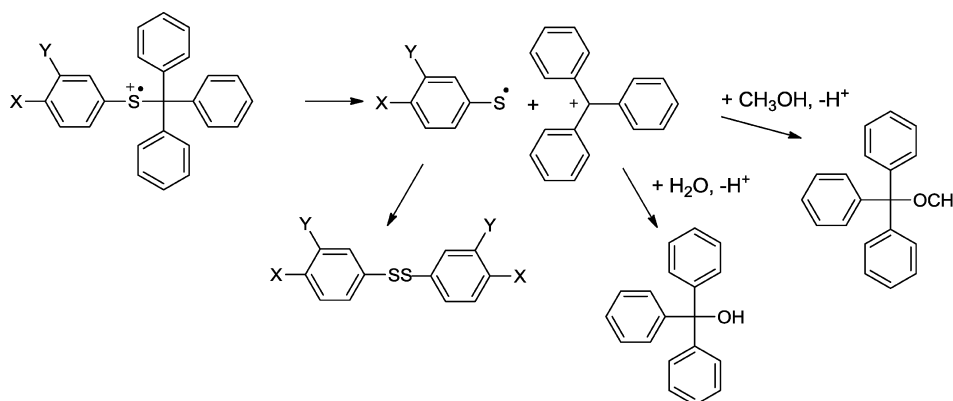
The structure of photoproducts formed can reasonably be rationalized on the basis of the formation of the radical cations **1^{•+}–5^{•+}** followed by the unimolecular cleavage of the C–S bond (eq 1).¹⁴ This process leads to the trityl cation and the arylsulfonyl radical (Scheme 3). The cations can then react with adventitious water in CH_3CN and CH_2Cl_2 to form the alcohols¹⁵ or with CH_3OH to give methyl triphenylmethyl ether in $\text{CH}_2\text{Cl}_2/\text{CH}_3\text{OH}$. Dimerization of arylsulfonyl radicals leads to diaryl disulfides.

The yields of the fragmentation products, referred to the initial amount of substrate, are reported in Table 1. The sensitizer is completely consumed during the photolysis; thus, the yields of the fragmentation products indicate an almost quantitative oxidation of the sulfides by the phenanthridinium radical cation (reaction b in Scheme 1). As expected, the yields of diaryl disulfides (Table 1) are about half of that of the triphenylmethanol or methyl triphenylmethyl ether.

Laser Flash Photolysis Studies. By laser photolysis ($\lambda_{\text{exc}} = 355 \text{ nm}$) of N_2 saturated CH_3CN solutions of sulfides **1–4** (0.01 M) and **MeOP⁺** ($1.6 \times 10^{-4} \text{ M}$), broad and intense absorption bands with maxima in the 530–630 nm region of the spectrum depending on the substrate were detected after the laser pulse. The same bands were also observed after laser photolysis of N_2 saturated solutions of sulfides **2** and **3** and

Scheme 1. Photochemical Generation of Radical Cations **1^{•+}–5^{•+}** by **MeOP⁺**



Scheme 2. Fragmentation Products in the Photooxidation of Sulfides 1–5 by MeOP⁺Scheme 3. C–S Bond Cleavage of Radical Cations 1^{•+}–5^{•+}Table 1. Products and Yields Formed in the Photooxidation of Aryl Triphenylmethyl Sulfides (1–5) Sensitized by MeOP^{•+}^a

Sulfide	Solvent	Products (Yield %) ^b	
		R=H	R=CH ₃
1 X=Y=OCH ₃	CH ₃ CN	19.8	10.0
2 X=OCH ₃ , Y=H	CH ₃ CN	16.9	8.6
	CH ₂ Cl ₂	18.2	8.5
3 X=CH ₃ , Y=H	CH ₂ Cl ₂ /CH ₃ OH 1:1	17.5	8.3
	CH ₃ CN	19.0	10.2
	CH ₂ Cl ₂	19.5	9.5
	CH ₂ Cl ₂ /CH ₃ OH 1:1	20.0	9.0
4 X=Y=H	CH ₃ CN	17.4	8.5
5 X=Br, Y=H	CH ₃ CN	17.8	9.0

^a[Sulfide] = 2.5–25 × 10^{−3} M, [MeOP^{•+}] = 0.5–2.5 × 10^{−3} M under nitrogen. Molar ratio sulfides/MeOP^{•+} = 5:1. ^bYields are referred to the initial amount of substrate. The error is ±5%.

MeOP^{•+} in CH₂Cl₂ or CH₂Cl₂/CH₃OH 1:1. These bands can be assigned to the radical cations 1^{•+}–4^{•+}^{7,8,16} formed by oxidation of sulfides 1–4 by the phenanthridine radical cation (P^{•+}) produced after N–O bond fragmentation in the MeOP^{•+} excited state.¹² The λ_{max} values for the radical cations 1^{•+}–4^{•+} are reported in Table 2. Absorption spectra are not modified by the presence of oxygen, thus confirming the cationic nature of the transients.

Table 2. Maximum Absorption Wavelengths (λ_{max}) and Decay Rate Constants (k_f) of Aryl Triphenylmethyl Sulfide Radical Cations (1^{•+}–5^{•+}) and Rate Constants for the Buildup of Triphenylmethyl Cation (k_b) Determined by LFP in the Photooxidation of 1–5 with MeOP^{•+}PF₆[−] (λ_{exc} = 355 nm) in N₂-Saturated CH₃CN

	λ _{max} (nm) ^a	k _f (s ^{−1}) ^b	k _b (s ^{−1}) ^c
1 ^{•+} X=Y=OCH ₃	625	4.4×10 ⁴	4.8×10 ⁴
2 ^{•+} X=OCH ₃ Y=H	610	2.0×10 ⁵	1.8×10 ⁵
3 ^{•+} X=CH ₃ Y=H	590	3.1×10 ⁶	3.2×10 ⁶
4 ^{•+} X=Y=H	530	9.5×10 ⁶	1.0×10 ⁷
5 ^{•+} X=Br Y=H	n.d.	>3×10 ⁷	>3×10 ⁷

^aFrom LFP experiments (λ_{exc} = 355 nm) in N₂-saturated CH₃CN. [Sulfide] = 1.0 × 10^{−2} M, [MeOP^{•+}PF₆[−]] = 8.8 × 10^{−4} M. ^bDecay rate constants recorded at the maximum of absorption of the radical cation.

^cBuildup rate constants of trityl cations recorded at 430 nm.

The time-evolution of the absorption spectra showed a slow first-order decay of the radical cations coupled with the growth of the absorption at 400–430 nm assigned to the formation of the trityl cation (C₆H₅)₃C⁺.¹¹ In the LFP experiment with the MeOP^{•+}/2 system a residual absorption is also observed at 520 nm which can be assigned to 4-CH₃OC₆H₄S[•].¹⁸

As an example, the time-resolved spectra of the LFP experiment with the 2/MeOP^{•+} system in CH₃CN are reported in Figure 1. Time resolved spectra for the 1/MeOP^{•+}, 3/MeOP^{•+}, and 4/MeOP^{•+} systems are shown in Figures S1–S3 in the Supporting Information. The results of the LFP experi-

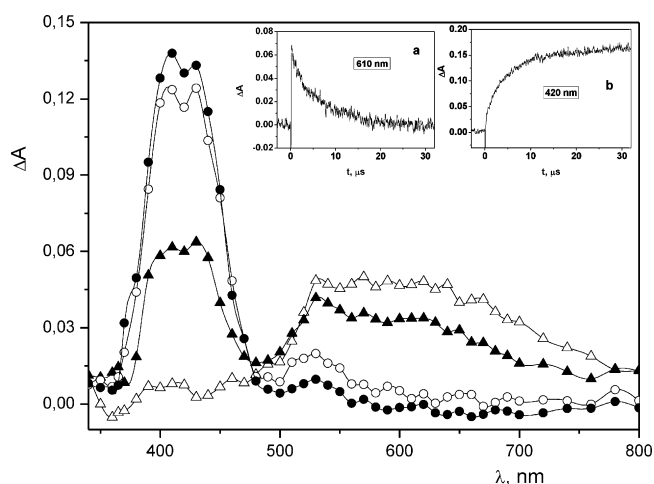


Figure 1. Time-resolved absorption spectra of the $\text{MeOP}^+ (1.6 \times 10^{-4} \text{ M})/4\text{-CH}_3\text{OC}_6\text{H}_4\text{SC}(\text{C}_6\text{H}_5)_3 (2) (1.0 \times 10^{-2} \text{ M})$ system in N_2 -saturated CH_3CN recorded 0.16 (Δ), 1.8 (\blacktriangle), 12 (\circ), and 32 (\bullet) μs after the laser pulse. Inset: (a) decay kinetics recorded at 610 nm; (b) buildup kinetics recorded at 420 nm.

ments with the $4/\text{MeOP}^+$ system have already been reported in a previous study.⁷ Similar time-resolved spectra have been observed after laser photolysis of N_2 saturated solutions of sulfides **2–3** and MeOP^+ in CH_2Cl_2 or $\text{CH}_2\text{Cl}_2/\text{CH}_3\text{OH}$ 1:1 (Figures S5–S8 in the Supporting Information). In the latter solvent, the buildup of the trityl cation is followed by its fast decay within 3 μs because of the reaction with the nucleophilic CH_3OH solvent (see insets b of Figures S6 and S8, Supporting Information).

While the time-resolved spectra of the $\text{MeOP}^+/\mathbf{1–4}$ systems resulted similar, different features were observed in the time-resolved spectra of the $\text{MeOP}^+/\mathbf{5}$ system. Upon laser excitation of a solution of $\text{MeOP}^+ (1.6 \times 10^{-4} \text{ M})$ and **5** ($1.0 \times 10^{-2} \text{ M}$) in N_2 -saturated CH_3CN , an intense absorption band at 410 nm and a less intense band at 510 nm were detected just after the laser pulse (Figure S4 in the Supporting Information). The two bands can be assigned respectively to the trityl cation and the sulphenyl radical $4\text{-BrC}_6\text{H}_4\text{S}^{\bullet 19}$ produced after C–S bond cleavage in $\mathbf{5}^{\bullet+}$. Clearly, the fragmentation rate of the radical cation $\mathbf{5}^{\bullet+}$ is so fast that the process takes place within the laser pulse. Thus, the radical cation is not observed but only the species produced in the fragmentation.

In conclusion, LFP experiments confirm the results of the steady-state photolysis suggesting that the decay of $\mathbf{1}^{\bullet+}–\mathbf{5}^{\bullet+}$ is due to the C–S bond cleavage with formation of trityl cations and the arylsulphenyl radicals ArS^{\bullet} . The latter species can be only observed in the LFP experiment with the $\text{MeOP}^+/\mathbf{2}$ system (see Figure 1, 12 μs after the laser pulse) due to the relatively strong absorption of $4\text{-CH}_3\text{OC}_6\text{H}_4\text{S}^{\bullet}$ ($\lambda_{\text{max}} = 520 \text{ nm}$, $\epsilon = 6.3 \times 10^3 \text{ M}^{-1} \text{ s}^{-1}$)¹⁸ and with the $\text{MeOP}^+/\mathbf{5}$ system where it is formed immediately after the laser pulse. The other arylsulphenyl radicals are characterized by low extinction coefficients, and their absorptions do not emerge in the spectra.²⁰

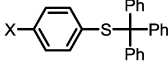
The rates of fragmentation of the aryl triphenylmethyl sulfide radical cations $\mathbf{1}^{\bullet+}–\mathbf{4}^{\bullet+}$ were determined by following either the decay kinetics (k_f) at the λ_{max} of the radical cations (Table 2) or the increase of absorbance at 430 nm due to the formation of the triphenylmethyl cation (k_b). In all cases, the decay kinetics followed first-order laws in accordance with an unimolecular fragmentation process. The rate of fragmentation for $\mathbf{5}^{\bullet+}$ was too high, and only a lower limit rate constant ($k_f > 3 \times 10^7 \text{ s}^{-1}$)

Table 3. Decay Rate Constants of the Aryl Triphenylmethyl Sulfide Radical Cations $\mathbf{2}^{\bullet+}–\mathbf{3}^{\bullet+}$ (k_f) and Buildup Rate Constants for the Triphenylmethyl Cation (k_b) in Different Solvents at 25 °C

$\text{X}-\text{C}_6\text{H}_4-\text{SC}(\text{C}_6\text{H}_5)_3$	Solvent	$k_f (10^5 \text{ s}^{-1})$	$k_b (10^5 \text{ s}^{-1})$
$\mathbf{2}^{\bullet+}$ X=OCH ₃	CH ₃ CN	2.0	1.8
	CH ₂ Cl ₂	8.6	8.6
	CH ₂ Cl ₂ /CH ₃ CN 1:1	3.3	3.8
	CH ₂ Cl ₂ /CH ₃ CN 3:1	4.0	4.8
	CH ₂ Cl ₂ /CH ₃ CN 9:1	6.8	7.0
	CH ₂ Cl ₂ /CH ₃ CN 95:5	8.8	10
	CH ₂ Cl ₂ /CH ₃ OH 1:1	3.6	n.d. ^a
	CH ₂ Cl ₂ /CH ₃ OH 3:1	5.1	n.d. ^a
	CH ₂ Cl ₂ /CH ₃ OH 9:1	8.5	n.d. ^a
	CH ₂ Cl ₂ /CH ₃ OH 95:5	8.8	10
$\mathbf{3}^{\bullet+}$ X=CH ₃	CH ₃ CN	31	32
	CH ₂ Cl ₂	89	114
	CH ₂ Cl ₂ /CH ₃ CN 1:1	32	44
	CH ₂ Cl ₂ /CH ₃ CN 3:1	53	78
	CH ₂ Cl ₂ /CH ₃ CN 9:1	70	92
	CH ₂ Cl ₂ /CH ₃ CN 95:5	83	110
	CH ₂ Cl ₂ /CH ₃ OH 1:1	38	44
	CH ₂ Cl ₂ /CH ₃ OH 3:1	59	56
	CH ₂ Cl ₂ /CH ₃ OH 9:1	78	79

^aAccurate rate determination is prevented by the fast decay of the cation in the presence of CH_3OH .

Table 4. Peak Oxidation Potentials (E_p) and C–S BDE of Sulfides 2–4 and C–S BDFEs of Sulfide Radical Cations $2^{\bullet+}$ – $4^{\bullet+}$

	E_p^a	C–S BDE (neutral substrates) ^b	C–S BDFE (radical cations) ^b
2 X=OCH ₃	1.30	24.9	-10.2
3 X=CH ₃	1.48	26.1	-13.2
4 X=H	1.56 ^c	30.0 ^c	-13.6 ^d

^aPeak oxidation potentials E_p (V vs SCE in CH₃CN) from cyclic voltammetry. ^bkcal mol⁻¹. ^cValues from ref 7. ^dThe value reported in ref 7 was recalculated using a more recent value (0.21 V vs SCE) for the reduction potential of triphenylmethyl cation (ref 24).

can be given. All the rate constants measured in CH₃CN at 25 °C are reported in Table 2.

The solvent effect on the C–S fragmentation process in $2^{\bullet+}$ and $3^{\bullet+}$ has been investigated by measuring the decay rate constants for the radical cations $2^{\bullet+}$ and $3^{\bullet+}$ (k_f) and the rate constants for the formation of the trityl cation (k_b) in CH₃CN and CH₂Cl₂ and in the solvent mixtures CH₃CN/CH₂Cl₂ and CH₃OH/CH₂Cl₂. All of the rate constants are reported in Table 3.

Theoretical Calculations. Neutral Sulfides. DFT calculations, carried out by using the Gaussian 03 package,²² at the B3P86/6-311+G(d,p)//B3P86/6-311+G(d,p) level of theory have been carried out for the neutral sulfides 2 and 3 in order to determine the C–S BDEs (the C–S BDE of 4 is available in the literature⁷). From these values, it is possible to estimate the C–S bond dissociation free energies (BDFEs) for the sulfide radical cations $2^{\bullet+}$ to $3^{\bullet+}$ by a thermochemical cycle^{7,8,23} (details in the Supporting Information).

The B3P86 functional was chosen because it is reported to be applied with reasonable success to the calculations of BDE values for a variety of C–X bonds,^{25,26} including C–S bonds.²⁶ It should also be noted that even though DFT methods may underestimate absolute BDE values, this should not affect the relative BDE values,^{26c} which are those for which we are mostly concerned. The calculated C–S BDEs of 2–4 are reported in Table 4, together with the BDFEs of the corresponding radical cations obtained by the thermochemical cycle using the C–S BDEs for the neutral sulfides 2–4 corrected for the entropic factor, the peak oxidation potentials of the sulfides reported in Table 4, and the reduction potential of the leaving triphenylmethyl carbocation (0.21 V vs SCE) available from the literature.²⁴

Since we are dealing with conformationally flexible molecules, before starting the BDEs calculation, all of the available conformations for the molecule and the radicals formed in the C–S scission process have to be found. To this end, a systematic conformational search was carried out, at the semiempirical PM3 level of theory,²⁷ by using the Conformer Search Module available in the Spartan 5.01 package.²⁸ All of the conformers found were optimized again, first at the B3LYP/6-31G level of theory and then at the higher B3P86/6-311+G(d,p) level of theory. The number of conformers found was four for 2 and two for 3. Only one conformer was found for each radical fragment.

In all of the calculations, the keywords integral (grid=ultrafine) scf=tight were used. For open-shell (radical) species, spin contamination due to states of multiplicity higher than the doublet state, was negligible since the expectation value $\langle S^2 \rangle$ of the total spin operator S^2 was, in all cases, within 5% of the expectation value for a doublet (0.75). Harmonic vibrational frequencies were calculated at the B3P86/6-311+G(d,p) level of theory to confirm that the stationary points found

correspond to local minima and to obtain the zero-point vibrational energy (ZPVE) corrections. For the ZPVE a scale factor of 0.9845 was used.²⁹ When more than one conformer was found for a given compound, its energy ($E_{el} + E_{ZPVE}$) to be used in the BDEs calculation, was obtained by Boltzmann averaging the energy ($E_{el} + E_{ZPVE}$) of all the corresponding minima. In the Supporting Information are reported the Cartesian coordinates, the electronic energy, and the zero-point vibrational energy of all the minima found.

Sulfide Radical Cations. DFT calculations were performed for sulfide radical cations $2^{\bullet+}$ – $3^{\bullet+}$ with the aim of obtaining the geometry of the minima, charges and spin distributions. The calculations were carried out at the B3LYP/6-311G(d,p)//B3LYP/6-311G(d,p) level of theory, the same one that was already used in a previous work on similar sulfide radical cations.^{8,30}

The starting geometries for the energy minimization of each radical cation were those of the corresponding neutral sulfide. Harmonic vibrational frequencies were calculated at the B3LYP/6-311G(d,p) level of theory to confirm that the stationary points found correspond to local minima. For all the radical cations, spin contamination due to states of multiplicity higher than the doublet state was negligible since the expectation value $\langle S^2 \rangle$ of the total spin operator S^2 was, in all cases, within 5% of the expectation value for a doublet (0.75). Two minima for $2^{\bullet+}$ and only a minimum for $3^{\bullet+}$ were found. The atomic charges were obtained by natural population analysis (NPA).³¹ Unpaired electron spin densities were calculated using the Mulliken population analysis.

In all of the energy minimum conformations of $2^{\bullet+}$ and $3^{\bullet+}$ the three phenyl rings of the trityl group are not coplanar. The geometry of the two conformers found for radical cation $2^{\bullet+}$ are very similar, differing only for the dihedral angle of the methoxy group (180° and 0°). The less stable conformer is only 0.26 kcal/mol above the most stable one. The most stable conformer of $2^{\bullet+}$ and the conformer at the minimum of energy of $3^{\bullet+}$ are shown in Figure 2.

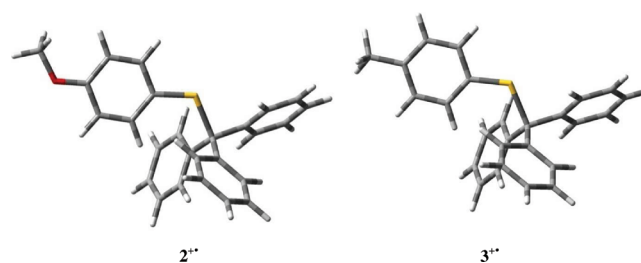


Figure 2. Most stable conformer for 4-MeOC₆H₄SC(C₆H₅)₃^{•+} ($2^{\bullet+}$) and conformer at the minimum of energy of 4-MeC₆H₄SC(C₆H₅)₃^{•+} ($3^{\bullet+}$).

In Table 5 are displayed NPA charges and spin density values obtained for the most stable conformers of radical cations $2^{\bullet+}$ and $3^{\bullet+}$, partitioned for the different structural components of the radical cations defined in Figure 3.

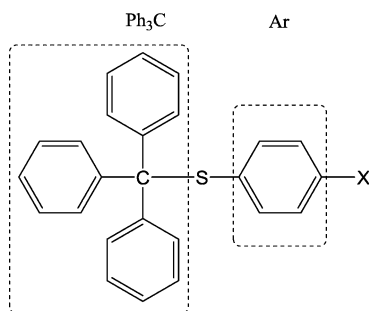


Figure 3. Structural components of aryl triphenylmethyl sulfide radical cations.

Table 5. NPA Charges (q_{NPA}) and Spin Densities for the Most Stable Conformers of Radical Cations $2^{\bullet+}$ and $3^{\bullet+}$

		Ph ₃ C	S	Ar	X
$2^{\bullet+}$	q_{NPA}	0.1400	0.5437	0.3903	−0.074
$2^{\bullet+}$	spin	0.0455	0.4307	0.4079	0.1160
$3^{\bullet+}$	q_{NPA}	0.1936	0.5803	0.1385	0.0877
$3^{\bullet+}$	spin	0.0774	0.5013	0.4070	0.0143

From the data reported in Table 5, it can be noted that NPA charges and spin populations in both $2^{\bullet+}$ and $3^{\bullet+}$ are mainly localized on the sulfur atom. The spin density is also relatively high on the arylsulfenyl ring and comparable for the two radical cations. Charge delocalization in the arylsulfenyl ring is much higher in $2^{\bullet+}$ than in $3^{\bullet+}$. This can be attributed to the methoxy substituent which is able to stabilize the positive charge by an electron releasing effect more efficiently than the methyl group.

In the attempt to identify a possible transition state for the C–S bond cleavage in the radical cations we have stepwise elongated the C–S bond in the radical cations starting from the energy minimum conformations. For each bond length we have partially optimized the geometry. In the optimization process the C–S bond length was kept fixed at a given value, whereas all the other degrees of freedom were allowed to relax. By increasing the C–S bond distance by 0.1 Å steps, we observed an initial increase of the energy of the system followed by a decrease at longer C–S distances (Table 6 and Table 7, for $2^{\bullet+}$ and $3^{\bullet+}$, respectively, and Figure 4). For each radical cation, the

Table 6. Energy Values (E and E_{rel}) Calculated for the Most Stable Conformer of Radical Cation $4\text{-MeOC}_6\text{H}_4\text{SC}(\text{C}_6\text{H}_5)_3^{\bullet+}$ ($2^{\bullet+}$) as a Function of the C–S Bond Distance

C–S distance, Å	E , au	E_{rel} , kcal/mol
1.96954	−1477.4396609	0.0000
2.06954	−1477.4391159	0.3420
2.16954	−1477.4382580	0.8804
2.26954	−1477.4378033	1.1657
2.28890 ^a	−1477.4377912 ^a	1.1733 ^a
2.36954	−1477.4380284	1.0244
2.56954	−1477.4402328	−0.3589

^aTransition state.

Table 7. Energy Values (E and E_{rel}) Calculated for the Conformer of Radical Cation $4\text{-MeC}_6\text{H}_4\text{SC}(\text{C}_6\text{H}_5)_3^{\bullet+}$ ($3^{\bullet+}$) as a Function of the C–S Bond Distance

C–S distance, Å	E , au	E_{rel} , kcal/mol
1.98407	−1402.2043135	0.0000
2.08407	−1402.2039104	0.2529
2.18407	−1402.2034192	0.5612
2.22968 ^a	−1402.2033518 ^a	0.6035 ^a
2.28407	−1402.2034536	0.5396
2.38407	−1402.2042226	0.0571
2.48407	−1402.2056275	−0.8245
2.58407	−1402.2074183	−1.9483

^aTransition state.

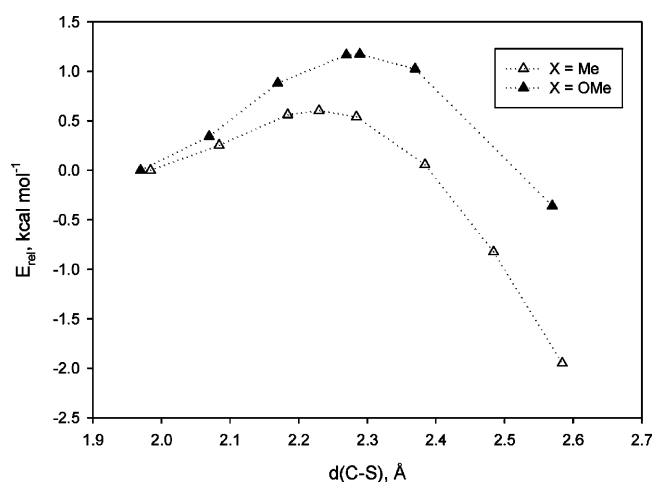


Figure 4. Plot of E_{rel} vs the C–S bond distances ($d(\text{C–S})$) for $2^{\bullet+}$ (▲) and $3^{\bullet+}$ (Δ).

geometry corresponding to the maximum energy value was optimized (opt=TS) to the nearest transition state. Each stationary point found was characterized by a frequency calculation and one imaginary frequency was found, thus confirming that the stationary point found is a saddle point. Furthermore, the normal mode corresponding to the imaginary frequency was animated by using the visualization program Molden.³² In this way it was verified that the displacements composing the mode corresponds to the C–S bond fragmentation process.

In Tables 8 and 9 are displayed the NPA charges and spin density values obtained for the optimized structures of radical cations $2^{\bullet+}$ and $3^{\bullet+}$ obtained by increasing the C–S bond distance and for the TS, partitioned for the different structural components defined in Figure 3.

DISCUSSION

The study of the C–S bond fragmentation in aryl triphenylmethyl sulfide radical cations has provided important information on the quantitative aspects of the electronic effects of arylsulfenyl ring substituents on the C–S bond cleavage in *tert*-alkyl aryl sulfide radical cations.

Theoretical calculations, carried out for $2^{\bullet+}$ and $3^{\bullet+}$, indicated for $2^{\bullet+}$ the presence of two energy minimum conformations very similar from both geometric and energetic points of view, while only one conformer at the minimum of energy was found for $3^{\bullet+}$. As shown in Figure 2, in both $2^{\bullet+}$ and $3^{\bullet+}$, due to the steric encumbrance of the trityl group, the C–S bond cannot be

Table 8. NPA Charges (q_{NPA}) and Spin Densities for the Optimized Structures of Radical Cation $2^{+\bullet}$

C–S distance, Å	NPA charges				spin population			
	Ph ₃ C	S	Ar	OCH ₃	Ph ₃ C	S	Ar	OCH ₃
1.96954	0.1400	0.5437	0.3903	−0.0740	0.0455	0.4307	0.4079	0.1160
2.06954	0.2066	0.4943	0.3769	−0.0778	0.0338	0.4510	0.4021	0.1131
2.16954	0.2834	0.4396	0.3599	−0.0828	0.0195	0.4764	0.3947	0.1093
2.26954	0.3678	0.3797	0.3410	−0.0885	0.0044	0.5042	0.3863	0.1051
2.28890 ^a	0.3848	0.3676	0.3373	−0.0897	0.0011	0.5098	0.3847	0.1043
2.36954	0.4570	0.3162	0.3216	−0.0948	−0.0097	0.5320	0.3771	0.1007
2.56954	0.6285	0.1927	0.2859	−0.1071	−0.0032	0.5619	0.3510	0.0903

^aTransition state.Table 9. NPA Charges (q_{NPA}) and Spin Densities for the Optimized Structures of Radical Cation $3^{+\bullet}$

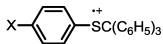
C–S distance, Å	NPA charges				spin population			
	Ph ₃ C	S	Ar	CH ₃	Ph ₃ C	S	Ar	CH ₃
1.98407	0.1936	0.5803	0.1385	0.0877	0.0774	0.5013	0.4070	0.0143
2.08407	0.2576	0.5292	0.1270	0.0863	0.0570	0.5242	0.4049	0.0138
2.18407	0.3316	0.4723	0.1118	0.0843	0.0339	0.5520	0.4010	0.0132
2.22968 ^a	0.3683	0.4444	0.1040	0.0833	0.0233	0.5653	0.3986	0.0128
2.28407	0.4137	0.4100	0.0943	0.0819	0.0111	0.5812	0.3953	0.0124
2.38407	0.5020	0.3438	0.0751	0.0791	−0.0045	0.6071	0.3859	0.0115
2.48407	0.5921	0.2768	0.0549	0.0762	−0.0018	0.6211	0.3702	0.0104
2.58407	0.6726	0.2162	0.0377	0.0735	0.0029	0.6307	0.3569	0.0096

^aTransition state.

perpendicular to one of the aromatic rings of the trityl moiety in a conformation most suitable for the C–S bond cleavage (the empty carbon p orbital formed in the cleavage is perfectly suited for an efficiently overlap with the π system) like those observed for aryl cumyl sulfide radical cations.⁸ The NPA charges and spin populations in $2^{+\bullet}$ and $3^{+\bullet}$ are mainly localized on the sulfur atom and on the arylsulfenyl ring (Table 5). It is interesting to note that NPA charges and spin populations are less localized on the trityl group of $2^{+\bullet}$ and $3^{+\bullet}$ with respect to the cumyl group in the **b** conformations of cumyl phenyl sulfide radical cations (4-X-C₆H₄C(CH₃)₂SC₆H₅^{•+}, X = H, CH₃, OCH₃).⁸ This difference can be reasonably attributed to the electron releasing arylsulfenyl ring substituents in $2^{+\bullet}$ and $3^{+\bullet}$ which are able to stabilize the positive charge reducing the electron density in the same ring.

From the kinetic data for the fragmentation of radical cations $1^{+\bullet}$ – $5^{+\bullet}$ in CH₃CN reported in Table 2, it can be immediately noted that the C–S bond cleavage rates are very sensitive to the nature of the substituent. As expected, the rates increase by decreasing the electron-donating power of the substituent, that is by decreasing the stability of the radical cations. An increase of about 200 times in fragmentation rate is observed on going from the 3,4-dimethoxy-substituted radical cation $1^{+\bullet}$ to the unsubstituted one $4^{+\bullet}$. The 3.4 kcal/mol difference in BDFE between $4^{+\bullet}$ and $2^{+\bullet}$ (Table 4) is associated to a substantial difference in ΔG^\ddagger (2.3 kcal/mol, see Table 10). This situation is much different from what observed in aryl cumyl sulfide radical cations where the C–S bond cleavage rates were insensitive to the nature of the substituent.⁸ Thus, the effect of substituents on the C–S bond cleavage process is significantly greater when they are introduced in the arylsulfenyl ring, where most of the charge and spin density is localized, than in an aromatic ring of the *tert*-alkyl group.⁸ In this respect, a key role on the relative magnitude of the fragmentation rate constants seems to be played by the effect of the substituents on the stabilization of the aryl sulfide radical cation. The stabilizing effect of electron-

Table 10. Activation Free Energies (ΔG^\ddagger), Free Energies (ΔG°), and Reorganization Energies for the C–S Bond Cleavage Sulfide Radical Cations $2^{+\bullet}$ – $4^{+\bullet}$

	ΔG^\ddagger ^{a,b}	ΔG° ^a	λ ^a
$2^{+\bullet}$ X=OCH ₃	8.9	−10.2	54.1
$3^{+\bullet}$ X=CH ₃	7.3	−13.2	52.3
$4^{+\bullet}$ X=H	6.6	−13.6	49.9

^aIn kcal mol^{−1}. ^bCalculated from the Eyring eq 3 using the k_f values reported in Table 2 and a collision frequency (Z) value of 6×10^{11} M^{−1} s^{−1}.

donating arylsulfenyl ring substituents is much higher than that exerted by the same substituents in the *tert*-alkyl group. Accordingly, the decrease in the oxidation potential observed by introducing a methoxy group in the arylsulfenyl ring (0.26 V, see Table 4) is much higher than that (0.07 V) found when the same substituent is introduced in the cumyl ring of aryl cumyl sulfides.⁸

Important information on the energetics of the C–S bond cleavage in aryl sulfide radical cations has been provided, for the first time, by DFT calculations. We increased the C–S distance by 0.1 Å steps in the radical cations $2^{+\bullet}$ and $3^{+\bullet}$ starting from the energy minimum conformations and calculated the energy of the optimized structures. It was found that the increase of the C–S bond distance led to an initial increase of the energy of the system followed by a decrease at longer C–S distances (Tables 6–7).³³ Thus, with this procedure (see above), we were able to identify the transition states for the C–S fragmentation process in the two radical cations. As predicted for the highly exergonic C–S bond cleavage processes in $2^{+\bullet}$ and $3^{+\bullet}$ (see Table 10), the transition states are reached quite early along the reaction coordinate and a relatively small increase of the C–S

bond distance is observed. In line with the early TS, the C–S bond cleavage rates are very sensitive to the ability of the substituent to stabilize the positive charge in the starting radical cations.

If we compare the TS of the two systems, it can be noted that the C–S bond distance and the energy relative to the starting conformer (E_{rel}) for 4-MeOC₆H₄SC(C₆H₅)₃^{•+} (**2**^{•+}) are higher than those calculated for 4-MeC₆H₄SC(C₆H₅)₃^{•+} (**3**^{•+}) (Figure 4). The degree of elongation of the C–S bond as measured by the increase of the C–S bond in the TS is ca. 16% of the initial bond length for **2**^{•+} and ca. 12% for **3**^{•+}. The higher E_{rel} value found for **2**^{•+} is in accordance with the lower rate of C–S fragmentation found for this radical cation. Although the difference in the E_{rel} of the two TS (0.6 kcal/mol) is not high enough to account for the observed differences in the C–S bond cleavage rates (ΔG^\ddagger = 1.6 kcal/mol in MeCN and 1.45 kcal/mol in CH₂Cl₂) it should be considered that calculations are referred to vacuum and enthalpic and entropic solvent effects might be responsible for the discrepancy.

Interesting results have been obtained from the analysis of the solvent effects on the C–S fragmentation process, investigated by following both the decay kinetics at the λ_{max} for the radical cations **2**^{•+} and **3**^{•+} (k_f) and the buildup rate constants for the formation of the triphenylmethyl cation (k_b) in different solvents (CH₃CN and CH₂Cl₂ and in the solvent mixtures CH₃CN/CH₂Cl₂ and CH₃OH/CH₂Cl₂). From the kinetic data reported in Table 3, it can be readily noted that the rate of C–S bond cleavage regularly increase by decreasing the polarity of the solvent. Accordingly, the C–S bond cleavage rates increase from $2 \times 10^5 \text{ s}^{-1}$ to $8.6 \times 10^5 \text{ s}^{-1}$ for **2**^{•+} and from $3 \times 10^6 \text{ s}^{-1}$ to ca. $1 \times 10^7 \text{ s}^{-1}$ for **3**^{•+} on going from the more polar CH₃CN to the less polar CH₂Cl₂ solvent. In the solvent mixtures CH₃CN/CH₂Cl₂ and CH₃OH/CH₂Cl₂ a regular increase of the fragmentation rates can be observed by increasing the relative amount of CH₂Cl₂. It is possible to rationalize the effect of the solvent polarity on the C–S fragmentation rates by considering that in aryl triphenylmethyl sulfide radical cations most of the charge is localized in the ArS moiety of the radical cation, as indicated by the results of DFT calculations (Table 5). This implies that such charge has to be transferred to the triphenylmethyl group in the final products. In the TS of the C–S bond cleavage the charge is more delocalized than in the starting radical cation as clearly shown from the data of Tables 8 and 9. The NPA charge localized on the triphenylmethyl group increase from 0.14 to 0.38 for **2**^{•+} and from 0.19 to 0.37 for **3**^{•+} on going from the starting radical cation to the transition states. Thus, a more polar solvent should stabilize the initial conformation more efficiently than the TS, increasing the barrier for the C–S fragmentation process. A decrease of the cleavage reactivity in radical cations by increasing the solvent polarity has been already observed in the fragmentation of tetraphenylethane radical cations.³⁵

The results of the solvent effects on the C–S bond cleavage of aromatic sulfide radical cations are instead different from those found in the C–C bond cleavage of bicumyl radical cations where the fragmentation rates are practically unaffected by changing the solvent polarity.³⁶ The absence of solvent effects on the C–C bond cleavage rates was interpreted by considering that all the charge is localized in a cumyl ring and remains in that ring after the C–C bond cleavage.⁹

Since DFT calculations have shown a significant delocalization of the charge and spin density on going from the reactant to the TS of the C–S fragmentation process of aryl

triphenylmethyl sulfide radical cations, we have analyzed how this great extent of delocalization is reflected in the reorganization energy value (λ) of the C–S bond cleavage. To this purpose we have treated the kinetic data for the fragmentation of radical cations **2**^{•+}–**4**^{•+} in terms of the Marcus equation (eq 2),³⁷ where ΔG^\ddagger is the activation free energy of the reaction, calculated by the Eyring equation (eq 3), replacing k_f with the values reported in Table 2 and Z as $6 \times 10^{11} \text{ M}^{-1} \text{ s}^{-1}$.³⁸ ΔG° is the free energy variation in the same reaction (C–S BDFE given in Table 4), and λ is the reorganization energy required for the fragmentation process.

$$\Delta G^\ddagger = (\lambda/4)(1 + \Delta G^\circ/\lambda)^2 \quad (2)$$

$$\Delta G^\ddagger = RT \ln(Z/k_f) \quad (3)$$

The values of ΔG^\ddagger and ΔG° (kcal mol^{−1}) are reported in Table 10. In the same table are also reported the λ values for the same reactions obtained from eq 4, which is derived from eq 2.

$$\lambda = 2\Delta G^\ddagger - \Delta G^\circ + 2[(\Delta G^\ddagger)^2 - \Delta G^\ddagger \times \Delta G^\circ]^{1/2} \quad (4)$$

Looking at the data in Table 10, it can be noted that the λ values obtained from the three reactions are similar, providing an average value of $52 \pm 2 \text{ kcal mol}^{-1}$ that can be reasonably taken as the reorganization energy for the C–S bond cleavage in aryl triphenylmethyl sulfide radical cations. This result, taken together with the λ value determined for the same process in aryl cumyl sulfide radical cations (43.7 kcal/mol),⁸ clearly indicates that a large reorganization energy is an intrinsic characteristic of the C–S bond fragmentation process of aryl sulfide radical cations. The higher λ value determined for the C–S bond cleavage in aryl triphenylmethyl sulfide radical cations suggests that a larger degree of charge transfer from ArS to the *tert*-alkyl group (greater extent of internal and solvent reorganization) should occur in the TS of the C–S bond cleavage in aryl triphenylmethyl sulfide radical cations with respect to aryl cumyl sulfide radical cations.

CONCLUSIONS

A significant variation of the C–S bond cleavage rates in aryl triphenylmethyl sulfide radical cations can be produced by changing the arylsulfenyl ring substituent or the reaction medium. Fragmentation rates decrease by increasing the electron-releasing properties of the arylsulfenyl ring substituent, that is by increasing the stability of the radical cations. This situation is much different from what observed in aryl cumyl sulfide radical cations where the C–S bond cleavage rates were very little sensitive to the nature of the substituent. These results have been rationalized by considering that the effect of the substituents on the stabilization of the aryl sulfide radical cation are significantly higher when they are introduced in the arylsulfenyl ring, where most of the charge and spin density is localized, than in the *tert*-alkyl group. For the first time, the structure, relative energies, spin and charge distribution of the transition states for the C–S bond cleavage in aryl sulfide radical cations have been calculated. The charge is more localized in the starting radical cation than in the transition state; therefore, a more polar solvent result in a decrease in the C–S bond cleavage rates compared to a less polar solvent.

■ EXPERIMENTAL SECTION

Starting Materials. Aryl triphenylmethyl sulfides 1–5 were prepared by acid-catalyzed reaction of the commercially available aryl-substituted thiophenol with triphenylmethanol as reported in the literature.³⁹ Compounds 1–3 were characterized by ¹H NMR, ¹³C NMR and HRMS (ESI-TOF) analysis. Compound 4 was synthesized and characterized in a previous study.⁷ Compound 5 was characterized according to the spectral data reported in the literature.⁴⁰ *N*-Methoxyphenanthridinium hexafluorophosphate was prepared according to a literature procedure.¹² CH₃CN (spectrophotometric grade) was distilled over CaH₂. CH₂Cl₂ (spectrophotometric grade) was distilled over P₂O₅. CH₃OH (spectrophotometric grade) was used as received.

Spectral Data of Substrates 1–3. *3,4-Dimethoxyphenyl Triphenylmethyl Sulfide (1).* ¹H NMR (300 MHz, CDCl₃): δ 3.47 (s, 3H), 3.80 (s, 3H), 6.31 (d, *J* = 2 Hz, 1H), 6.58 (d, *J* = 8 Hz, 1H), 6.74 (dd, *J* = 8 Hz, 2 Hz, 1H), 7.18–7.39 (m, 15H). ¹³C NMR (300 MHz, CDCl₃): δ 55.3, 55.8, 70.7, 110.6, 118.9, 124.6, 126.6, 127.6, 129.4, 130.1, 144.7, 148.1, 149.6. HRMS (ESI-TOF): calcd C₂₇H₂₄O₂S + Na⁺ [M + Na]⁺ 435.1395, found 435.1458.

4-Methoxyphenyl Triphenylmethyl Sulfide (2). ¹H NMR (300 MHz, CDCl₃): δ 3.70 (s, 3H), 6.52–6.90 (m, 4H); 7.17–7.42 (m, 15H). ¹³C NMR (300 MHz, CDCl₃): δ 55.2, 70.8, 113.7, 124.4, 126.6, 127.6, 130.0, 137.8, 144.7, 160.1. HRMS (ESI-TOF): calcd C₂₆H₂₂OS + Na⁺ [M + Na]⁺ 405.1289, found 405.1231.

4-Methylphenyl Triphenylmethyl Sulfide (3). ¹H NMR (300 MHz, CDCl₃): δ 2.21 (s, 3H), 6.82–6.83 (m, 2H), 7.17–7.42 (m, 17H). ¹³C NMR (300 MHz, CDCl₃): δ 21.1, 70.6, 126.6, 127.6, 128.9, 130.1, 130.6, 135.1, 138.0, 144.7. HRMS (ESI-TOF): calcd C₂₆H₂₂S + Na⁺ [M + Na]⁺ 389.1340, found 389.1355.

Steady-State Photolysis. Photooxidation reactions were carried out in a photoreactor equipped with 2–4 lamps (360 nm; 14 W each). A 1 mL solution containing the substrate 1–5 (5–25 × 10^{−3} M) and MeOP⁺ (0.5–2.5 × 10^{−3} M) (sulfide/MeOP⁺ molar ratio = 5:1) in N₂-saturated CH₃CN, CH₂Cl₂, or CH₂Cl₂/CH₃OH 1:1, was placed in a quartz cell and irradiated for 5–10 min. An internal standard (diphenylmethane) was added, and the mixtures were analyzed by ¹H NMR and HPLC. The following products were identified by comparison with authentic specimens: triphenylmethanol, methyl triphenylmethyl ether, bis(3,4-dimethoxyphenyl) disulfide, bis(4-methoxyphenyl) disulfide, bis(4-methylphenyl) disulfide, diphenyl disulfide, bis(4-bromophenyl) disulfide, protonated phenanthridine, and methanol. The photoproducts were quantified by HPLC and ¹H NMR. The material balance was always satisfactory (>90%). Blank experiments, carried out by irradiating the solutions in the absence of MeOP⁺, did not show product formation in any cases.

Laser Flash Photolysis. Excitation wavelength of 355 nm (Nd:YAG laser, Continuum, third harmonic, pulse width ca. 7 ns and energy <3 mJ per pulse) was used in nanosecond flash photolysis experiments. The transient spectra were obtained by a point-to-point technique, monitoring the change of absorbance (ΔA) after the laser flash at intervals of 5–10 ns over the spectral range 300–800 nm, averaging at least 10 decays at each wavelength. Nitrogen was bubbling through the solution. All measurements were carried out at 22 ± 2 °C unless otherwise indicated. The experimental error on the decay rate constants was estimated to be ±10%.

Theoretical Calculations. The calculations were run on the 22TFlops Linux Cluster “Matrix” consisting of 330 nodes dual-socket quad-core Opteron CPU each, with Infiniband DDR as main interconnect and a shared filesystem based on Luster 1.8.4 via IB. Located at the supercomputing center “CASPUR” (Rome).

■ ASSOCIATED CONTENT

● Supporting Information

Time-resolved absorption spectra after LFP of the MeOP⁺/1, MeOP⁺/3, MeOP⁺/4, and MeOP⁺/5 systems in CH₃CN; time-resolved absorption spectra after LFP of the MeOP⁺/2, MeOP⁺/3 systems in CH₂Cl₂ and CH₂Cl₂/CH₃OH 1:1; cyclic

voltammetry; C–S BDFEs of radical cations 2^{•+}–3^{•+}, Cartesian Coordinates, energies, ZPVE from DFT calculations for neutral sulfides 2 and 3, for triphenylmethyl and arylsulfenyl radicals and for radical cations 2^{•+} and 3^{•+} conformers at the minimum of energy; NPA charges and Mulliken spin densities for radical cations 2^{•+} and 3^{•+}; Cartesian coordinates, energies, NPA Charges and Mulliken spin densities for TS of the C–S bond cleavage in the radical cations 2^{•+} and 3^{•+}. This material is available free of charge via the Internet at <http://pubs.acs.org>.

■ AUTHOR INFORMATION

Corresponding Author

*E-mail: osvaldo.lanzalunga@uniroma1.it; paolo.mencarelli@uniroma1.it; dgiacco@unipg.it.

■ ACKNOWLEDGMENTS

Financial support from the Ministero dell’Istruzione, dell’Università e della Ricerca (MIUR) is gratefully acknowledged. We thank Prof. Enrico Baciocchi for helpful discussions and Prof. Ruggero Caminiti (Chemistry Department, Sapienza Università di Roma) for generously letting us use his computer time at the supercomputing center “CASPUR”.

■ REFERENCES

- (1) (a) Lanzalunga, O.; Lapi, A. *J. Sulfur Chem.* **2011**, DOI: 10.1080/17415993.2011.619536. (b) Park, J.; Morimoto, Y.; Lee, Y.-M.; Nam, W.; Fukuzumi, S. *J. Am. Chem. Soc.* **2011**, 133, 5236. (c) Khenkin, A. M.; Leitun, G.; Neumann, R. *J. Am. Chem. Soc.* **2010**, 132, 11446. (d) Vorontsov, A. V. *Russ. Chem. Rev.* **2008**, 77, 909. (e) Huang, M. L.; Rauk, A. *J. Phys. Chem. A* **2004**, 108, 6222. (f) Glass, R. S. *Spec. Chem. Mag.* **2002**, 22, 34. (g) Tobien, T.; Cooper, W. J.; Nickelsen, M. G.; Pernas, E.; O’Shea, K. E.; Asmus, K.-D. *Environ. Sci. Technol.* **2000**, 34, 1286. (h) Glass, R. S. *Top. Curr. Chem.* **1999**, 205, 1. (i) *S-Centered Radicals*; Alfassi, Z. B., Ed.; Wiley: New York, 1999. (j) Bauld, N. L.; Aplin, J. T.; Yueh, W.; Loinaz, A. J. *Am. Chem. Soc.* **1997**, 119, 11381. (k) Goetz, M.; Rozwadowski, J.; Marciniak, B. *J. Am. Chem. Soc.* **1996**, 118, 2882. (l) Glass, R. S. *Xenobiotica* **1995**, 25, 637. (m) *Sulfur-Centered Reactive Intermediates in Chemistry and Biology*, NATO ASI Series A, Life Science; Chatgililoglu, C., Asmus, K.-D., Eds.; Plenum Press: New York, 1990. (n) Asmus, K.-D. *Acc. Chem. Res.* **1979**, 12, 436.
- (2) (a) Bobrowski, K.; Houee-Levin, C.; Marciniak, B. *Chimia* **2008**, 62, 728. (b) Schöneich, C.; Pogocki, D.; Hug, G. L.; Bobrowski, K. *J. Am. Chem. Soc.* **2003**, 125, 13700. (c) Butterfield, D. A.; Kanski, J. *Peptides* **2002**, 23, 1299. (d) Schöneich, C. *Arch. Biochem. Biophys.* **2002**, 397, 370. (e) Goto, Y.; Matsui, T.; Ozaki, S.; Watanabe, Y.; Fukuzumi, S. *J. Am. Chem. Soc.* **1999**, 121, 9497. (f) Miller, B. L.; Kuczera, K.; Schöneich, C. *J. Am. Chem. Soc.* **1998**, 120, 3345. (g) Bobrowski, K.; Hug, G. L.; Marciniak, B.; Miller, B. L.; Schöneich, C. *J. Am. Chem. Soc.* **1997**, 119, 8000. (h) Marciniak, B.; Hug, G. L.; Rozwadowski, J.; Bobrowski, K. *J. Am. Chem. Soc.* **1995**, 117, 127. (i) Ozaki, S.; Ortiz de Montellano, P. R. *J. Am. Chem. Soc.* **1995**, 117, 7056. (j) Kobayashi, S.; Nakano, M.; Kimura, T.; Schaap, P. *Biochemistry* **1987**, 26, 5019. (k) Watanabe, Y.; Numata, T.; Iyanagi, T.; Oae, S. *Bull. Chem. Soc. Jpn.* **1981**, 54, 1163.
- (3) (a) Peñeñory, A. B.; Argüello, J. E.; Puigatti, M. *Eur. J. Org. Chem.* **2005**, 10, 114. (b) Adam, W.; Argüello, J. E.; Peñeñory, A. B. *J. Org. Chem.* **1998**, 63, 3905. (c) Ioele, M.; Steenken, S.; Baciocchi, E. *J. Phys. Chem. A* **1997**, 101, 2979. (d) Baciocchi, E.; Lanzalunga, O.; Malandrucchio, S.; Ioele, M.; Steenken, S. *J. Am. Chem. Soc.* **1996**, 118, 8973. (e) Baciocchi, E.; Rol, C.; Scamosci, E.; Sebastiani, G. V. *J. Org. Chem.* **1991**, 56, 5498.
- (4) Venimadhavan, S.; Amarnath, K.; Harvey, N. G.; Cheng, J.-P.; Arnett, E. M. *J. Am. Chem. Soc.* **1992**, 114, 221.
- (5) (a) Baciocchi, E.; Gerini, M. F.; Lanzalunga, O.; Lapi, A.; Lo Piparo, M. G. *Org. Biomol. Chem.* **2003**, 1, 422. (b) Baciocchi, E.;

- Lanzalunga, O.; Pirozzi, B. *Tetrahedron* **1997**, *53*, 12287. (c) Baciocchi, E.; Lanzalunga, O.; Marconi, F. *Tetrahedron Lett.* **1994**, *35*, 9771. (d) Baciocchi, E.; Bietti, M.; Ioele, M.; Lanzalunga, O.; Steenken, S. In *Free Radicals in Biology and Environment*; Minisci, F., Ed.; Kluwer: Dordrecht, 1997. (e) Oae, S.; Mikami, A.; Matsuura, T.; Ogawa-Asada, K.; Watanabe, Y.; Fujimori, K.; Iyanagi, T. *Biochem. Biophys. Res. Commun.* **1985**, *131*, 567. (f) Watanabe, Y.; Oae, S.; Iyanagi, T. *Bull. Chem. Soc. Jpn.* **1982**, *55*, 188.
- (6) (a) Baciocchi, E.; Bietti, M.; Lanzalunga, O. *J. Phys. Org. Chem.* **2006**, *19*, 467. (b) Wang, L.; Seiders, J. R.; Floreancig, P. E. *J. Am. Chem. Soc.* **2004**, *126*, 12596. (c) Seiders, J. R.; Wang, L.; Floreancig, P. E. *J. Am. Chem. Soc.* **2003**, *125*, 2406. (d) Kumar, V. S.; Floreancig, P. E. *J. Am. Chem. Soc.* **2001**, *123*, 3842. (e) Baciocchi, E.; Bietti, M.; Lanzalunga, O. *Acc. Chem. Res.* **2000**, *33*, 243. (f) Schmittel, M.; Burghart, A. *Angew. Chem., Int. Ed. Engl.* **1997**, *36*, 2550. (g) Dinnocenzo, J. P.; Simpson, T. R.; Zuilhof, H.; Todd, W. P.; Heinrich, T. *J. Am. Chem. Soc.* **1997**, *119*, 987. (h) Dockery, K. P.; Dinnocenzo, J. P.; Farid, S.; Goodman, J. L.; Gould, I. R.; Todd, W. P. *J. Am. Chem. Soc.* **1997**, *119*, 1876. (i) Schepp, N. P.; Shukla, D.; Johnston, L. J.; Sarker, H.; Bauld, N. L. *J. Am. Chem. Soc.* **1997**, *119*, 10325. (j) Gaillard, E. R.; Whitten, D. G. *Acc. Chem. Res.* **1996**, *29*, 292. (k) Maslak, P. *Top. Curr. Chem.* **1993**, *168*, 1. (l) Todd, W. P.; Dinnocenzo, J. P.; Farid, S.; Goodman, J. L.; Gould, I. R. *Tetrahedron Lett.* **1993**, *34*, 2863. (m) Albini, A.; Fasani, E.; d'Alessandro, N. *Coord. Chem. Rev.* **1993**, *125*, 269. (n) Popielarz, R.; Arnold, D. R. *J. Am. Chem. Soc.* **1990**, *112*, 3068. (o) Dinnocenzo, J. P.; Farid, S.; Goodman, J. L.; Gould, I. R.; Todd, W. P.; Mattes, S. L. *J. Am. Chem. Soc.* **1989**, *111*, 8973.
- (7) Baciocchi, E.; Del Giacco, T.; Gerini, M. F.; Lanzalunga, O. *Org. Lett.* **2006**, *8*, 641.
- (8) Baciocchi, E.; Bettoni, M.; Del Giacco, T.; Lanzalunga, O.; Mazzonna, M.; Mencarelli, P. *J. Org. Chem.* **2011**, *76*, 573.
- (9) Maslak, P.; Vallombroso, T. M.; Chapman, W. H.; Narvaez, J. N. *Angew. Chem., Int. Ed. Engl.* **1994**, *33*, 73.
- (10) The effect of a methoxy substituent in the arylsulfenyl ring on the C–S bond cleavage in radical cations of aryl 1-methyl-1-arylethyl sulfides has been investigated.⁸ Slower rates were observed with respect to the radical cations of the unsubstituted phenyl sulfides, but unfortunately, the decrease was such that the comparison was possible only with the radical cation 4-CH₃O-C₆H₄C(CH₃)₂SC₆H₅^{•+} in which the charge and spin densities are mainly localized in the cumyl ring.
- (11) Faria, J. L.; Steenken, S. *J. Am. Chem. Soc.* **1990**, *112*, 1277.
- (12) Shukla, D.; Guanghua, L.; Dinnocenzo, J. P.; Farid, S. *Can. J. Chem.* **2003**, *81*, 744.
- (13) Baciocchi, E.; Crescenzi, C.; Lanzalunga, O. *Tetrahedron* **1997**, *53*, 4469. Elinson, M. N.; Simonet, J.; Wendt, H. *J. Electroanal. Chem.* **1993**, *350*, 117. Baciocchi, E.; Intini, D.; Piermattei, A.; Rol, C.; Ruzziconi, R. *Gazz. Chim. Ital.* **1989**, *119*, 649.
- (14) Baciocchi, E.; Fasella, E.; Lanzalunga, O.; Mattioli, M. *Angew. Chem., Int. Ed. Engl.* **1993**, *32*, 1071.
- (15) In acetonitrile, formation of alcohols by reaction of the stable tertiary cumyl, diphenylmethyl, diphenylethyl and triphenylmethyl carbocations with water (ca. 0.01 M in the spectrophotometric grade CH₃CN) was reported in previous steady state photolysis studies of the C–S fragmentation reactions of aryl sulfides^{7,8,16} and aryl sulfoxide radical cations.¹⁷ Acetamides deriving from the Ritter reaction with the solvent CH₃CN were instead formed from relatively less stable and less selective *tert*-butyl, 1-methylcyclopentyl, benzyl, and 1-phenylethyl carbocations.
- (16) Baciocchi, E.; Del Giacco, T.; Giombolini, P.; Lanzalunga, O. *Tetrahedron* **2006**, *62*, 6566.
- (17) Baciocchi, E.; Del Giacco, T.; Lanzalunga, O.; Mencarelli, P.; Procacci, P. *J. Org. Chem.* **2008**, *73*, 5675. Baciocchi, E.; Lanzalunga, O.; Lapi, A.; Maggini, L. P. *J. Org. Chem.* **2009**, *74*, 1805.
- (18) Riyad, M.; Naumov, S.; Hermann, R.; Brede, O. *Phys. Chem. Chem. Phys.* **2006**, *8*, 1697.
- (19) Ito, O.; Tamura, S.; Murakami, K.; Matsuda, M. *J. Org. Chem.* **1988**, *53*, 4758.
- (20) λ_{max} (C₆H₅S[•]) = 460 nm, $\epsilon = 2.6 \times 10^3 \text{ M}^{-1} \text{ s}^{-1}$.^{21a} λ_{max} (4-CH₃C₆H₄S[•]) = 485 nm, $\epsilon = 2.65 \times 10^3 \text{ M}^{-1} \text{ s}^{-1}$.^{21b} The ϵ values for 4-BrC₆H₄S[•] and 3,4-(CH₃O)₂C₆H₃S[•] are not available in the literature.
- (21) (a) Tripathi, G. N. R.; Sun, Q.; Armstrong, D. A.; Chipman, D. M.; Schuler, R. H. *J. Phys. Chem.* **1992**, *96*, 5344. (b) Hermann, R.; Dey, G. R.; Naumov, S.; Brede, O. *Phys. Chem. Chem. Phys.* **2000**, *2*, 1213.
- (22) Frisch, M. J.; Trucks, G. W.; Schlegel, H. B.; Scuseria, G. E.; Robb, M. A.; Cheeseman, J. R.; Montgomery, J. A., Jr.; Vreven, T.; Kudin, K. N.; Burant, J. C.; Millam, J. M.; Iyengar, S. S.; Tomasi, J.; Barone, V.; Mennucci, B.; Cossi, M.; Scalmani, G.; Rega, N.; Petersson, G. A.; Nakatsuji, H.; Hada, M.; Ehara, M.; Toyota, K.; Fukuda, R.; Hasegawa, J.; Ishida, M.; Nakajima, T.; Honda, Y.; Kitao, O.; Nakai, H.; Klene, M.; Li, X.; Knox, J. E.; Hratchian, H. P.; Cross, J. B.; Adamo, C.; Jaramillo, J.; Gomperts, R.; Stratmann, R. E.; Yazyev, O.; Austin, A. J.; Cammi, R.; Pomelli, C.; Ochterski, J. W.; Ayala, P. Y.; Morokuma, K.; Voth, G. A.; Salvador, P.; Dannenberg, J. J.; Zakrzewski, V. G.; Dapprich, S.; Daniels, A. D.; Strain, M. C.; Farkas, O.; Malick, D. K.; Rabuck, A. D.; Raghavachari, K.; Foresman, J. B.; Ortiz, J. V.; Cui, Q.; Baboul, A. G.; Clifford, S.; Cioslowski, J.; Stefanov, B. B.; Liu, G.; Liashenko, A.; Piskorz, P.; Komaromi, I.; Martin, R. L.; Fox, D. J.; Keith, T.; Al-Laham, M. A.; Peng, C. Y.; Nanayakkara, A.; Challacombe, M.; Gill, P. M. W.; Johnson, B.; Chen, W.; Wong, M. W.; Gonzalez, C.; and Pople, J. A., Gaussian 03, Revision D.02, Gaussian, Inc., Pittsburgh PA, 2003.
- (23) The C–S BDFE for the radical cation 4^{•+} reported in ref 7 (–12.3 kcal mol^{–1}) was recalculated using a more recent value for the reduction potential of triphenylmethyl cation (0.21 V vs SCE).²⁴
- (24) Fukuzumi, S.; Ohkubo, K.; Otera, J. *J. Am. Chem. Soc.* **2001**, *66*, 1450.
- (25) (a) Yao, X.-Q.; Hou, X.-J.; Jiao, H.; Wu, G.-S.; Xu, Y.-Y.; Xiang, H.-W.; Jiao, H.; Li, Y.-W. *J. Phys. Chem. A* **2002**, *106*, 7184. (b) Zhao, J.; Cheng, X.; Yang, X. *THEOCHEM* **2006**, *766*, 87. (c) Van Speybroeck, V.; Marin, G. B.; Waroquier, M. *ChemPhysChem* **2006**, *7*, 2205. (d) Su, X.-F.; Cheng, X.; Liu, Y.-G.; Li, Q. *Int. J. Quantum Chem.* **2007**, *107*, 515.
- (26) (a) Johnson, E. R.; Clarkin, O. J.; DiLabio, G. A. *J. Phys. Chem. A* **2003**, *107*, 9953. (b) Yao, X.-Q.; Hou, X.-J.; Jiao, H.; Xiang, H.-W.; Li, Y.-W. *J. Phys. Chem. A* **2003**, *107*, 9991. (c) Feng, Y.; Liu, L.; Wang, J.-T.; Huang, H.; Guo, Q.-X. *J. Chem. Inf. Comput. Sci.* **2003**, *43*, 2005.
- (27) Stewart, J. J. P. *J. Comput. Chem.* **1989**, *10*, 209.
- (28) Spartan 5.01, Wavefunction, Inc., Irvine, CA.
- (29) Merrick, J. P.; Moran, D.; Radom, L. *J. Phys. Chem. A* **2007**, *111*, 11683.
- (30) Baciocchi, E.; Gerini, M. F. *J. Phys. Chem. A* **2004**, *108*, 2332.
- (31) Reed, A. E.; Curtiss, L. A.; Weinhold, F. *Chem. Rev.* **1988**, *88*, 899.
- (32) Schaftenaar, G.; Noordik, J. H. Molden: a pre- and post-processing program for molecular and electronic structures. *J. Comput.-Aided Mol. Design* **2000**, *14*, 123.
- (33) A similar situation was encountered in the exothermic C–C bond scission of bicumyl radical cation where the calculated C–C bond distance in the TS and the barrier height of the dissociation were 1.75 Å and 2.3 kcal mol^{–1} (UHF values) or 1.81 Å and 1.6 kcal mol^{–1} (RHF values).³⁴
- (34) Camaioni, D. M. *J. Am. Chem. Soc.* **1990**, *112*, 9475.
- (35) Faria, J. L.; McClelland, R. A.; Steenken, S. *Chem.—Eur. J.* **1998**, *4*, 1275.
- (36) Maslak, P.; Chapman, W. H.; Vallombroso, T. M.; Watson, B. A. *J. Am. Chem. Soc.* **1995**, *117*, 12380.
- (37) Marcus, R. A. *Annu. Rev. Phys. Chem.* **1964**, *15*, 155.
- (38) Ebersson, L. *Electron Transfer Reactions in Organic Chemistry*; Springer Verlag: Berlin, 1986; Chapter 3.
- (39) Screttas, C. G.; Micha-Screttas, M. *J. Org. Chem.* **1977**, *42*, 1462.
- (40) Touaibia, M.; Desjardins, M.-A.; Provencal, A.; Audet, D.; Medard, C.; Morin, M.; Breau, L. *Synthesis* **2004**, 2283.